Hindawi Publishing Corporation
EURASIP Journal on Image and Video Processing
Volume 2008, Article ID 970353, 9 pages
doi:10.1155/2008/970353

Research Article

Edge-Detected Guided Morphological Filter for Image Sharpening

T. A. Mahmoud and S. Marshall (EURASIP Member)

Department of Electronic and Electrical Engineering, University of Strathclyde, 204 George Street, Glasgow G1 1XW, UK

Correspondence should be addressed to S. Marshall, s.marshall@eee.strath.ac.uk

Received 26 February 2008; Revised 23 July 2008; Accepted 6 November 2008

Recommended by Ferran Marques

A new edge-guided morphological filter is proposed to sharpen digital images. This is done by detecting the positions of the edges and then applying a class of morphological filtering. Motivated by the success of threshold decomposition, gradient-based operators are used to detect the locations of the edges. A morphological filter is used to sharpen these detected edges. Experimental results demonstrate that the performance of these detected edge deblurring filters is superior to that of other sharpener-type filters.

1. INTRODUCTION

Pictures or images play an important role as a mass communication medium. The tremendous volume of optical information and the need for its processing and transmission have paved the way to image processing by digital computers [1].

Image sharpening has played an important role in image processing since the beginning of the digital image revolution [2]. Thus, many well-known techniques for image sharpening exist today and are readily available in most commercial software packages. Moreover, sharpening of images is becoming increasingly important as closed-circuit television (CCTV) becomes more pervasive and the identification of people for security reasons is of international concern.

Edge detection is a fundamental tool, which is commonly used in many image processing applications to obtain information from the images and frames. This process detects boundaries between objects and background in the image.

Digital image enhancement techniques are concerned with improving the quality of the digital image. The principal objective of enhancement techniques is to produce an image which is better and more suitable than the original image for a specific application. Digital image enhancement is usually done simultaneously with detection of features such as edges and peaks. Linear filters have been used to solve many image enhancement problems. Throughout the history of image processing, linear operators have been the dominating filter class. This is triggered by the computational efficiency of linear filtering algorithms. Despite the elegant linear system theory, not all image sharpening problems can be satisfactorily addressed through the use of linear filters. Many researchers now hold the view that it is not possible to obtain major breakthroughs in image sharpening without resorting to nonlinear methods. Nowadays, a new understanding has emerged that linear approaches are not well suited or even fail to solve problems involving geometrical aspects of the image. Thus, there is a need for nonlinear geometric approaches, and selectivity in image sharpening is the key to its success. A powerful nonlinear methodology that can successfully address the image sharpening problem is mathematical morphology [3].

Morphological processing techniques result in changes to signals and images based on shape. Very simple morphological operations such as dilations and erosions may be used to increase the slope of an intensity gradient and hence, make the image sharper. The fact that morphological operations can enhance edges is not in doubt. However, these operations must be applied selectively only at the edges and not over the entire image. Application of standard edge detectors, such as Prewitt and Sobel, results in a detection of edges based on thresholding. On the other hand, application of adaptive edge detectors can provide a better and effective performance. This means that the edges can stop and start sporadically. In this new approach, the problem of edge detection is regarded as a classification problem in pattern recognition. Sharpening only at these locations gives unpredictable results. A better approach, taken in this paper, is to enhance the image at edges more closely associated with the grayscale intensity values. This new concept is achieved by means of threshold decomposition, which will be explained later. Edges must be sharpened only with respect to their principal direction. Therefore, edge directions must be estimated accurately in addition to identification of edges locations.

In this paper, a novel approach is proposed for effectively sharpening blurred images. The scheme presented is based on edge detection. If the edges can be detected and their positions are correctly located in the image, then it is feasible to increase the contrast of these edges by invoking a morphological filter only at these locations. The proposed filter is significantly interesting for its novel theory and improved results. Experimental results demonstrate that the performance of these detected edge deblurring filters is superior to that of other sharpener-type filters. This paper is an extension to the authors' work in [4]. The use of diagonal operators and the detection of thin edges are introduced in this paper.

Section 2 introduces the concept of threshold decomposition and the method used for edge detection. Morphological filtering for image sharpening is explained in Section 3. Section 4 will present in detail the proposed sharpening filter. Then, this filter is tested on several examples, and its performance is compared with that of traditional sharpener-type filters. Edge detection morphological of Gaussian filter will be described in Section 5. Finally, Section 6 contains some concluding remarks.

2. BACKGROUND

Edge detection has been increasing popular for its usage in most image processing applications. Edge detection is by far the most common approach for detecting meaningful discontinuities in gray level images. Intuitively, an edge is a set of connected pixels that lie on the boundary between two regions. Consequently, due to the blurring effect, edges are more closely as having a *ramp-like* profile. The slope of the ramp is inversely proportional to the degree of blurring in the edge. Each pixel in an image has gradient edge amplitude as well as direction. A new concept is presented by detecting the edge locations by means of threshold decomposition.

2.1. Threshold decomposition

Threshold decomposition is a powerful theoretical tool, which is used in nonlinear image analysis. Many filter techniques have been shown to "commute with thresholding." This means that the image may be decomposed into a series of binary levels, each of which may be processed separately. These binary levels can, then, be recombined to produce the final grayscale image with identical pixel values to those produced by grayscale processing. Hence, a grayscale operation may be replaced by a series of equivalent binary operations. In many cases, the design of the binary operator is much more straightforward than its grayscale counterpart. The first threshold decomposition framework for image processing was introduced by Fitch et al. [5]. This was capable of modeling a wide range of filters based on rank ordering such as the median and weighted order statistics (WOS) operators. It was also capable of modeling linear FIR filters with positive weights. The framework was limited to model low-pass filters or "smoothers."

More recently, the framework was modified by Arce [6], Paredes and Arce [7]. This modification introduced the ability to model both linear and nonlinear filters with negative as well as positive filter weights. Its effect opened up the possibility to model high-pass and band-pass filters as well as low-pass filters.

Motivated by this success, an image sharpening technique is developed, in this paper, and implemented through a framework of threshold decomposition. The framework is given here, for more details; the reader may refer to the cited papers.

Consider an integer-valued set of samples $X_1, X_2, \ldots, X_N$ forming the signal $X = [X_1, X_2, \ldots, X_N]$, where $X_i \in \{-M, \ldots, -1, 0, 1, \ldots, M\}$. The threshold decomposition of X amounts to decompose this signal into $2M$ binary signals $x^{-M+1}, \ldots, x^0, \ldots, x^M$, where the ith element of x^m is defined by (1) as follows:

$$x_i^m = \begin{cases} 1 & \text{if } X_i \geq m, \\ -1 & \text{if } X_i < m. \end{cases} \tag{1}$$

The above threshold decomposition is reversible, such that if a set of threshold signals is given, each of the samples in X can be exactly reconstructed as shown in (2) as follows:

$$X_\mathrm{i} = \frac{1}{2} \sum_{m=-M+1}^{M} x_i^m. \tag{2}$$

Thus, an integer-valued discrete-time signal has a unique threshold signal representation and vice versa.

2.2. Edge detection

Edge detection is a fundamental tool, which is commonly used in many image processing applications. This process detects boundaries between different regions in the image. An edge detection filter can be used to improve the appearance of blurred images or video streams.

Since edge detection has been an active area of research for more than 40 years, many effective methods have been proposed such as gradient edge detectors (first derivative), zero crossing (second derivative), Laplacian of Gaussian (LOG), and Gaussian edge detectors [8].

Some sophisticated edge detection techniques have recently been introduced in the literature. Law et al. [9] design fuzzy rules for edge detection; however, this method requires rather large and complicated rules. Methods based on the maximum objective function are proposed in [10] to

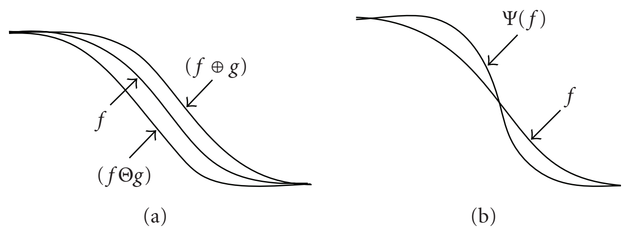

Figure 1: (a) Dilation and erosion of a signal f (by a flat structuring element). (b) Contrast enhancement of f by switching between dilation and erosion using a sharpening filter ψ. The figure shows that switching between a dilation and erosion as defined by (7) results in an increase in gradient and hence, a contrast enhancement.

extract more accurate and thinner contours of the objects. Moreover, in the last few years, the application of the wavelet transform in image processing has received significant attention. Some very efficient wavelet-based multiscale edge detection algorithms have been proposed in [11]. Also, multiscale signal analysis may be combined with the wavelet transform to increase the reliability of edge detection [12]. It has been shown that genetic fuzzy clustering algorithms may be used to solve problems produced from low-level edges [13].

In spite of all these efforts, none of the proposed operators solve all of the problems in real world applications. They do not lead to satisfactory results when used as means of identifying locations at which to apply image sharpening. In this work, the enhancement is applied through a framework of threshold decomposition. This has two advantages: it reduces the edge detection to a simple binary process and it makes the estimation of edge direction straightforward. Edge detection and direction estimation may be carried out by identifying simple patterns, which are closely related to the Prewitt operator [14]. The operators are sometimes called compass operators because of their ability to determine gradient direction. The gradient is estimated in 8 possible directions (for a 3×3 mask) with a difference of 45° between each direction. The first four operators are shown as the four (3×3 mask) below, the other four can be obtained by applying a 45°-clockwise rotation. By using the 8 masks of the Prewitt operators, thick edges in the 8 directions can be detected as follows:

$$
\begin{aligned}
h_1 &= \begin{bmatrix} 1 & 1 & 1 \\ D_0 & D_1 & D_2 \\ -1 & -1 & -1 \end{bmatrix}, \qquad h_2 = \begin{bmatrix} D_0 & 1 & 1 \\ -1 & D_1 & 1 \\ -1 & -1 & D_2 \end{bmatrix}, \\
h_3 &= \begin{bmatrix} -1 & D_0 & 1 \\ -1 & D_1 & 1 \\ -1 & D_2 & 1 \end{bmatrix}, \qquad h_4 = \begin{bmatrix} -1 & -1 & D_0 \\ -1 & D_1 & 1 \\ D_2 & 1 & 1 \end{bmatrix},
\end{aligned} \tag{3}
$$

where $g = \{D_0, D_1, D_2\}$ is the structuring element used in the mathematical morphology. Section 3.2 will introduce the types of structuring elements used in this paper to process the input image in the morphological operations.

On the other hand, the 8 masks mentioned in [15] can be used to detect thin edges in the 8 directions. The first four operators are represented by the four (3×3 mask) shown below, the other four can be obtained by developing the negative of these matrices:

$$
\begin{aligned}
k_1 &= \begin{bmatrix} -1 & -1 & -1 \\ 1 & 1 & 1 \\ -1 & -1 & -1 \end{bmatrix}, \qquad k_2 = \begin{bmatrix} 1 & -1 & -1 \\ -1 & 1 & -1 \\ -1 & -1 & 1 \end{bmatrix}, \\
k_3 &= \begin{bmatrix} -1 & 1 & -1 \\ -1 & 1 & -1 \\ -1 & 1 & -1 \end{bmatrix}, \qquad k_4 = \begin{bmatrix} -1 & -1 & 1 \\ -1 & 1 & -1 \\ 1 & -1 & -1 \end{bmatrix}.
\end{aligned} \tag{4}
$$

With the aid of the threshold decomposition described above, and for each level, the edges are detected by searching for patterns of gray levels consistent with the 8 masks of the Prewitt operators for thick edges and the 8 masks mentioned in [15] for thin edges. Thus, the sharpening filter is applied only at these detected edges rather than all the pixels of the image.

It should be pointed out that the Prewitt filter masks are used here as a simple way to determine edges and their direction in the threshold decomposed image. They are convenient in that they have values of ± 1. Thus, they are not used to apply the Prewitt edge detector to the grayscale image, where it is acknowledged that the Prewitt edge detector is inferior to more modern edge detectors as mentioned earlier.

3. IMAGE SHARPENING BY MORPHOLOGICAL FILTERING

Mathematical morphology offers a unified and powerful approach to numerous image processing problems. One of the most appealing aspects of morphological image processing is addressing the image sharpening problem [3].

3.1. Introduction to mathematical morphology

Kramer and Bruckner [16] and then Lester et al. [17] define a nonlinear transformation for sharpening digitized grayscale images. The transformation replaces the gray-level value at a pixel either by the minimum or the maximum of the gray-level value in its neighborhood. The choice is dependent on which one is closer in value to the original gray-level intensity.

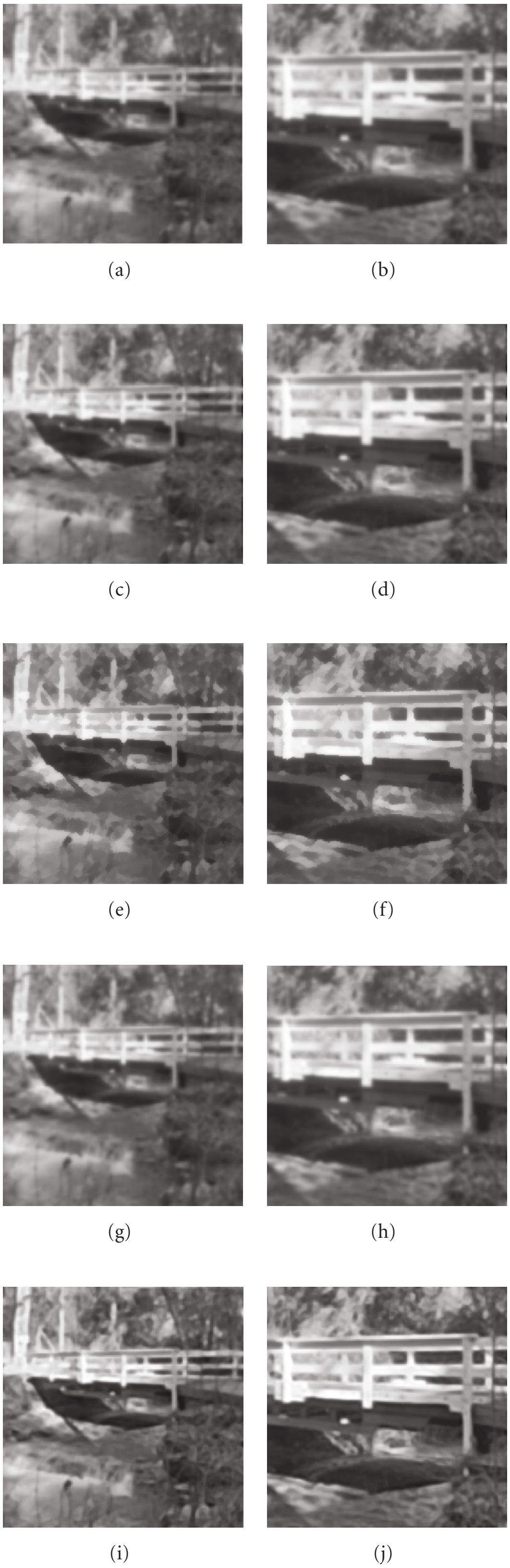

Figure 2: (a) Blurred bridge and zoomed-in version in (b). The result of the modified high-pass, LUM, QV, and the proposed edge-detected flat structuring element morphological filter are given in (c), (e), (g), and (i) along with their zoomed-in versions in (d), (f), (h), and (j), respectively.

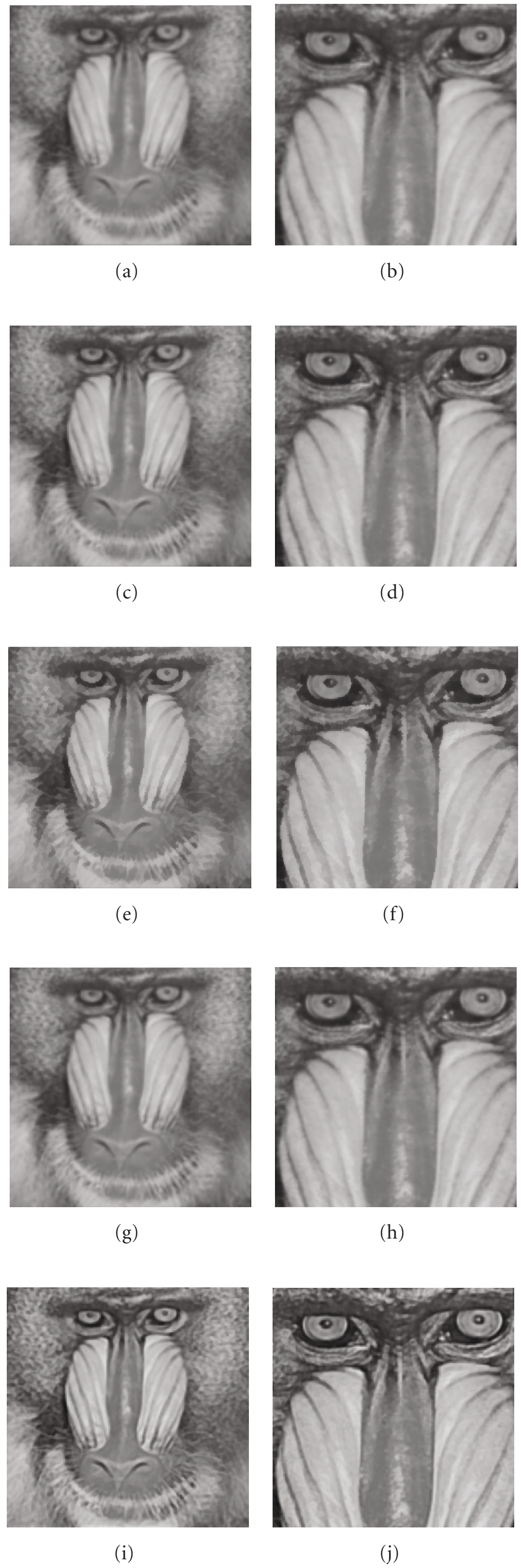

Figure 3: (a) Blurred Baboon and zoomed-in version in (b). The result of the modified high-pass, LUM, QV, and the proposed edge-detected flat structuring element morphological filter are given in (c), (e), (g), and (i) along with their zoomed-in versions in (d), (f), (h), and (j), respectively.

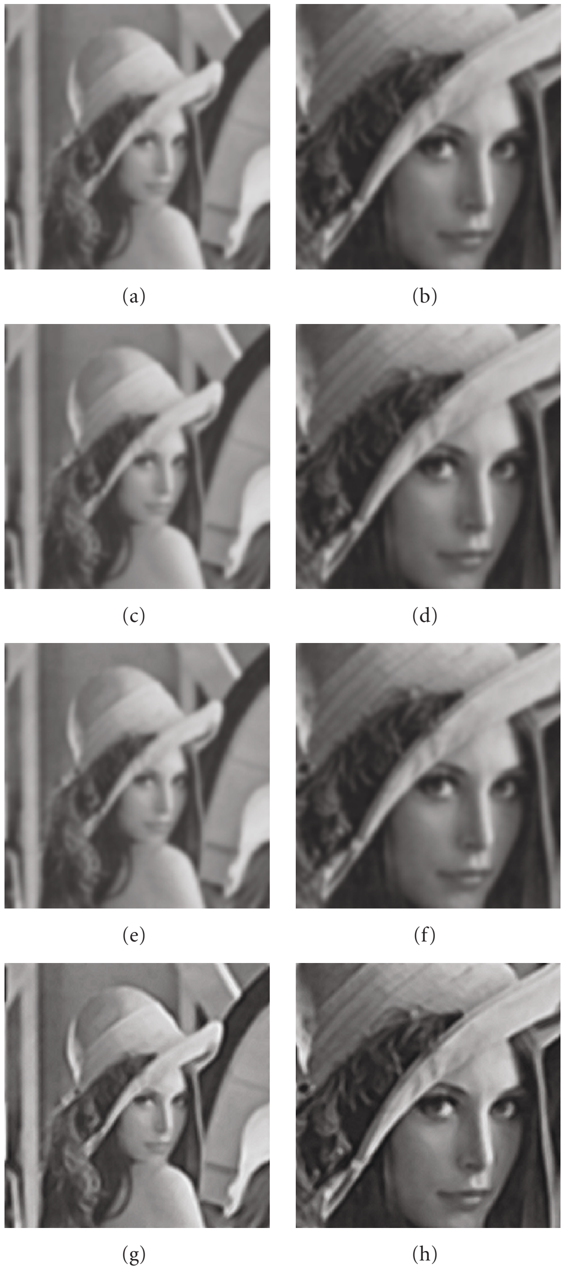

Figure 4: (a) Lenna image corrupted by 10% grain noise and blurred by a Gaussian filter and zoomed-in version in (b). The result of the modified high-pass, QWM, and the proposed edge-detected flat structuring element morphological filter are given in (c), (e), and (g) along with their zoomed-in versions in (d), (f), and (h), respectively.

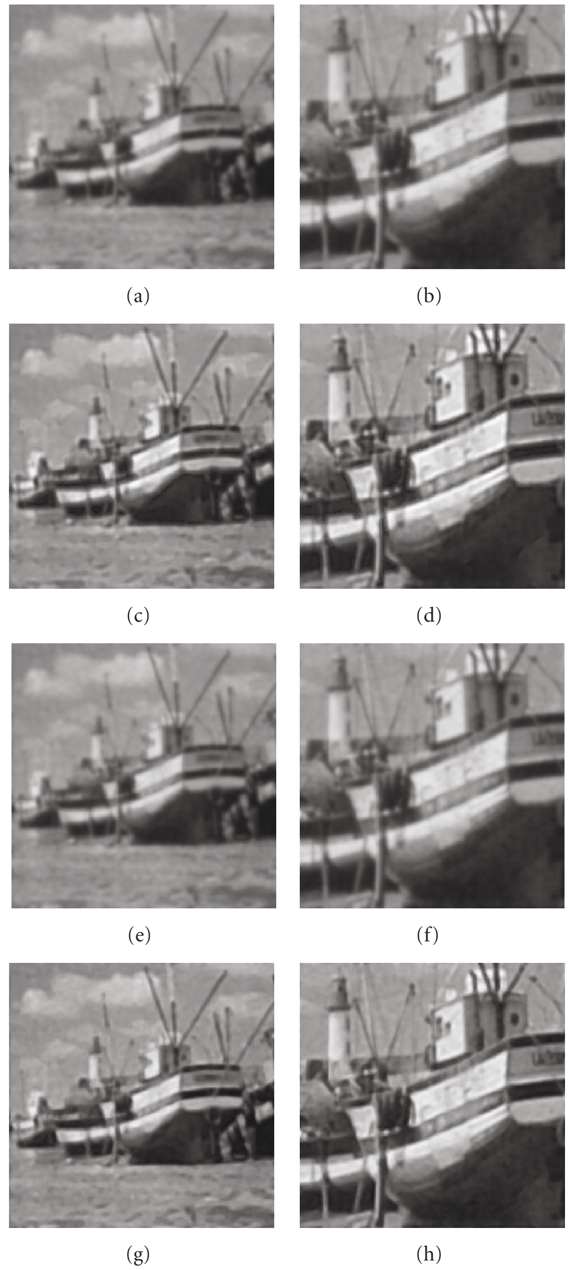

Figure 5: (a) Sailboat image corrupted by 10% grain noise and blurred by a Gaussian filter and zoomed-in version in (b). The result of the modified high-pass, QWM, and the proposed edge-detected flat structuring element morphological filter are given in (c), (e), and (g) along with their zoomed-in versions in (d), (f), and (h), respectively.

In mathematical morphology [18], the transformation which replaces the gray-level value at a pixel by the maximum of the gray-level value in its neighborhood is known as the grayscale dilation operator and is defined by (5) as follows:

$$(f \oplus g)(x) = \max_{\mu \in R^2}[f(\mu) + g(x - \mu)], \tag{5}$$

in which function $f(x)$, $f : x \in R^2 \rightarrow f(x) \in R$ is the original image, and $g(x), g : x \in R^2 \rightarrow g(x) \in R$ is the structuring element implicitly defining the weighted neighborhood.

Similarly, the transformation which replaces the gray-level value at a pixel by the minimum of the gray-level value in its neighborhood is known as the grayscale erosion operator and is defined by (6) as follows:

$$(f \,\Theta\, g)(x) = \min_{\mu \in R^2}[f(\mu) - g(\mu - x)]. \tag{6}$$

Note that the dilation operator is extensive: $(f \oplus g)(x) \geq f(x)$, and the erosion operator is antiextensive: $(f \Theta g)(x) \leq f(x)$.

3.2. Contrast enhancement

Consider a grayscale signal $f(x)$ and a structuring element g containing the origin, Kramer and Bruckner [16] and then redefined by Schavemaker et al. [19] used the following discrete nonlinear filter to enhance the local contrast of $f(x)$ by increasing its gradient as shown in (7):

$$\psi(f(x)) = \begin{cases} (f \oplus g)(x) & \text{if } f(x) \geq \dfrac{(f \oplus g)(x) + (f \Theta g)(x)}{2}, \\ (f \Theta g)(x) & \text{if } f(x) < \dfrac{(f \oplus g)(x) + (f \Theta g)(x)}{2}. \end{cases} \tag{7}$$

According to (7), the output of the filter depends on the relative magnitude of the original signal $f(x)$ as compared to the average of its eroded and dilated versions. If the original signal $f(x)$ is greater than or equal to this average, then the output of the filter ψ follows the dilation of $f(x)$, and if it is lower, then ψ follows its erosion. The dilation is carried out by a flat or concave structuring element and tends to be larger than the original signal close to the gradient. On the other hand, the erosion is lower than the original signal.

Figure 1 shows that the output value of this filter switches between the value of the dilation of $f(x)$ by $g(x)$ and the value of its erosion by $g(x)$. This switch causes the gradient of the signal to increase, which leads to a contrast enhancement [20].

This paper will focus on two types of structuring element in order to sharpen a grayscale image. Firstly, Kramer and Bruckner in [16] use flat structuring elements for sharpening digitized grayscale images, in this case, $g(x)$ could be $\{1, 1, 1\}$ or $\{2, 2, 2\}$, and so forth. Secondly, Schavemaker et al. in [19] have proved that all image operators using concave structuring elements have sharpening properties, in this case, $g(x)$ could be $\{1, 2, 1\}$ or $\{2, 3, 2\}$, and so forth. In this paper, it will be demonstrated that these two structuring elements have sharpening behavior, and that the flat structuring elements are slightly preferable to the parabolic concave structuring ones.

4. THE PROPOSED SHARPENING FILTER AND EXPERIMENTAL RESULTS

The sequence of applying the proposed filter will be explained before introducing the experimental results. First, the threshold decomposition method introduced in Section 2.1 is applied to the blurred image to produce a stack of binary images. At each level, a search is performed for the 16 possible edge directions as described in Section 2.2. Binary morphological operations of dilation and erosion are used to increase the contrast in the region and direction of the detected edges with the aid of a flat or concave structuring element [21]. The nonlinear discrete filter is thus used to sharpen only at detected edges, rather than the whole image.

The reader should note that while many standard morphological functions commute with thresholding, in this paper, the binary operations carried out contain a step which is conditional on the edge direction found at each level. This means that the overall process no longer commutes with thresholding, and therefore a single equivalent grayscale operation does not exist.

This section presents application results for the sharpening operator using a flat or concave structuring element in the discrete domain. The performance of the proposed filters is compared with a number of sharpener-type filters including high-pass sharpener, modified high-pass sharpener [22], and lower-upper-middle (LUM) filter [23]. Moreover, the performance of the proposed filter is compared with that of the optimum performance of two filters from the state-of-the-art in image sharpening. firstly, the quadratic weighted median (QWM) filter [24] which is an extension of the quadratic volterra (QV) filter [25]. Secondly, the proposed Bi-Laplacian of Gaussian (Bi-LOG) filter in [26], which is an extension of the Laplacian of Gaussian in the well-know Mach band illusion.

Three different measures, the normalized mean square error (NMSE), the structural similarity (SSIM) index [27], and the edge-based structural similarity (ESSIM) index [28], are used to give a quantitative evaluation on the filtering results.

The NMSE is calculated from the following formula:

$$\text{NMSE} = \frac{\sum_{i=-N/2}^{N/2} \sum_{j=-N/2}^{N/2} \left(I_{ij} - Y_{ij}\right)^2}{\sum_{i=-N/2}^{N/2} \sum_{j=-N/2}^{N/2} \left(I_{ij}\right)^2}, \tag{8}$$

where I_{ij} is the ideal image, Y_{ij} is the filtered image, and $N \times N$ is the size of the image. The best filter is characterized by achievement of the *lowest* NMSE.

Recently, SSIM was introduced under the assumption that human visual perception is highly adapted for extracting structural information from a scene. The SSIM is an alternative complementary framework for quality assessment based on the degradation of structural information. The best filter is characterized by achievement of the *highest* SSIM. The SSIM is described mathematically by (9) [27] as follows:

$$\text{SSIM}(i, j) = l(i, j) \times c(i, j) \times s(i, j). \tag{9}$$

SSIM includes three components: Luminance comparison $l(i, j)$, contrast comparison $c(i, j)$, and structure comparison $s(i, j)$.

Luminance comparison is defined by

$$l(i, j) = \frac{2\mu_{ij_I}\mu_{ij_Y} + C_1}{\mu_{ij_I}^2 + \mu_{ij_Y}^2 + C_1}, \tag{10}$$

where μ_{ij_I} and μ_{ij_Y} are the mean intensities of the ideal and the filtered images, respectively, and C_1 is a small constant that is included to avoid instability when the denominator is very close to zero.

Table 1: NMSE, SSIM, and ESSIM for different sharpener-type filters. For each image, the value in bold indicates the best filter with the *lowest* NMSE, the *highest* SSIM as well as the *highest* ESSIM.

Sharpener filter	Bridge			Baboon		
	NMSE	SSIM	ESSIM	NMSE	SSIM	ESSIM
Blur image	0.0238	0.6450	0.5152	0.0160	0.6559	0.5046
High-pass sharpener	0.0236	0.5254	0.3451	0.0158	0.5615	0.3408
Modified high-pass sharpener	0.0224	0.5629	0.3689	0.0148	0.6129	0.3930
LUM sharpener	0.0187	0.5979	0.4159	0.0139	0.6228	0.4543
QV	0.0227	0.5565	0.3769	0.0150	0.6123	0.4045
QWM	0.0228	0.5419	0.3636	0.0152	0.5864	0.3748
Bi-LOG	0.0402	0.6564	0.5285	0.0460	0.5857	0.4768
Sharpener filter proposed in [16]	0.0234	0.6537	0.5183	0.0158	0.6556	0.5160
Sharpener filter proposed in [18]	0.0219	0.6573	0.5013	0.0154	0.6578	0.5084
Prewitt edge detection with filter in [16]	0.0236	0.6524	0.5147	0.0157	0.6531	0.5121
Proposed concave structuring element	0.0149	**0.6751**	0.5298	0.0113	**0.7186**	**0.5347**
Proposed flat structuring element	**0.0146**	0.6745	**0.5312**	**0.0112**	0.7167	0.5307

Table 2: NMSE, SSIM, and ESSIM for different sharpener-type filters. For each image, the value in bold indicates the best filter with the *lowest* NMSE, the *highest* SSIM as well as the *highest* ESSIM.

Sharpener filter	Lenna			Sailboat		
	NMSE	SSIM	ESSIM	NMSE	SSIM	ESSIM
Blur image	0.0132	0.7222	0.6026	0.0145	0.6544	0.4742
Modified high-pass sharpener	0.0094	0.7716	0.6525	0.0110	0.7170	0.5502
QWM	0.0128	0.7309	0.6217	0.0138	0.6704	0.4981
Proposed EDMOG fiter	**0.0082**	**0.7848**	**0.6789**	**0.0100**	**0.7368**	**0.5759**

Contrast comparison is defined by

$$c(i, j) = \frac{2\,\sigma_{ij_I}\,\sigma_{ij_Y} + C_2}{\sigma_{ij_I}^2 + \sigma_{ij_Y}^2 + C_2}, \tag{11}$$

where σ_{ij_I} and σ_{ij_Y} are the contrast standard deviations of the ideal and the filtered images, respectively, and C_2 is a small constant that is included to avoid instability when the denominator is very close to zero.

Structure comparison is defined by

$$s(i, j) = \frac{\sigma_{ij_{IY}} + C_3}{\sigma_{ij_I}\,\sigma_{ij_Y} + C_3}, \tag{12}$$

where $\sigma_{ij_{IY}}$ is the correlation coefficient corresponding to the cosine of the angle between the images $I - \mu_{ij_I}$ and $Y - \mu_{ij_Y}$, and $C_3 = C_2/2$ is a small constant that is included to avoid instability when the denominator is very close to zero.

Chen et al. [28] found that the SSIM failed in measuring heavily blurred images. Based on this, an improved method was developed which is called edge-based structural similarity (ESSIM). ESSIM compares the edge information between the blocks of the filtered image and the original ones. Thus, the structure comparison $s(i, j)$ in (9) is replaced by the edge-based structure comparison $e(i, j)$. The best filter is characterized by achievement of the *highest* ESSIM. The ESSIM is described as follows [28]:

$$\text{ESSIM}(i, j) = l(i, j) \times c(i, j) \times e(i, j), \tag{13}$$

where $e(i, j)$ is the edge comparison and is defined by

$$e(i, j) = \frac{\sigma'_{ij_{IY}} + C_3}{\sigma'_{ij_I}\sigma'_{ij_Y} + C_3}, \tag{14}$$

where σ'_{ij_I} and σ'_{ij_Y} are the standard deviations of vectors D_I and D_Y, respectively, $\sigma'_{ij_{IY}}$ is the covariance of vectors D_I and D_Y, where D_I and D_Y represent the block edge direction histograms of the ideal and filtered images, respectively. Chen et al. used a nonoverlapping 8×8 block size.

Throughout the result section, the SSIM and ESSIM measures utilize the following parameter settings: $C_1 = 0.01$; $C_2 = 0.03$, the same as those used in [27, 28].

The proposed filter is tested on two examples shown. Figures 2 and 3(a) are the Gaussian blurred test images and zoomed-in versions in Figures 2 and 3(b). The results of the sharpened images after applying the modified high-pass, LUM, and QV sharpener are shown in Figures 2 and 3(c), 3(e), 3(g) along with their zoomed-in versions in Figures 2 and 3(d), 3(f), and 3(h), respectively. Figures 2 and 3(i) show the sharpened images after applying the proposed *flat structuring element morphological filter* on the detected edges, along with their zoomed-in versions in Figures 2 and 3(j), respectively. The resulting images of the proposed method are noticeably sharper. The horizontal and vertical fences in the bridge and the eyes and face details of the Baboon all have been enhanced.

Table 1 shows the NMSE, SSIM, and ESSIM as quantitative comparisons between the above-mentioned sharpening techniques. The output of each filter is evaluated by comparing its estimate to the original image.

5. EDGE DETECTION MORPHOLOGICAL OF GAUSSIAN AND EXPERIMENTAL RESULTS

In this section, the edge-detected guided morphological filter will be modified to sharpen degraded images having blurred edges and noisy surfaces. In this sharpening category, the proposed edge-detected guided morphological filter is combined with Gaussian smoothing. Consider (15),

$$G(r_g) = -e^{-r_g^2/2\sigma_g^2}, \tag{15}$$

where r_g is the Gaussian blur radius, and σ_g is the Gaussian standard deviation.

Convolving this function with an image results in image blur. Applying the proposed edge-detected guided morphological filter leads to a method referred to as the *edge detection morphological of a Gaussian* (EDMOG) filter.

The performance of the proposed EDMOG filter is compared with a number of sharpener-type filters including modified high-pass sharpener proposed in [22], and QWM proposed in [24].

As test images, the well-known *Lenna* and *Sailboat* images were used. Figures 4 and 5(a) are the test images corrupted by 10% grain noise and degraded by Gaussian blur. The zoomed-in versions are shown in Figures 4 and 5(b). The results of the sharpened image after applying the modified high-pass sharpener and the QWM are shown in Figures 4 and 5(c) and 5(e) along with their zoomed-in versions in Figures 4 and 5(d) and 5(f), respectively. Figures 4 and 5(g) show the sharpened image after applying the proposed EDMOG filter, with $r_g = 3.0$ pixels and $\sigma_g = 0.5$, and using flat structuring element morphological filter, along with their zoomed-in versions in Figures 4 and 5(h).

Table 2 shows the NMSE, SSIM, and ESSIM as quantitative comparisons between the above-mentioned sharpening techniques. The output of each filter is evaluated by comparing its estimate to the original image.

From the figures of the filtered images and the table of the NMSE, SSIM, and ESSIM, some conclusions are reached. Comparing the filtered images clearly indicates that the proposed EDMOG filter outperforms both the modified high-pass sharpener and the QWM filter in respect of grain noise removal, edge sharpening, and fine detail restoration. The NMSE, SSIM, and ESSIM tables demonstrate that the proposed EDMOG filter achieves the *lowest* NMSE and the *highest* SSIM and ESSIM.

6. CONCLUSIONS

In this paper, a new image sharpening filter based on morphological filters was presented. Edges are first detected through threshold decomposition. Then, the type of structuring element is chosen from the flat or the parabolic concave structuring elements. Both give good results, but the flat structuring element was found to perform slightly better. Thus, the threshold decomposition guided adaptive filters have the ability to sharpen a blurred image. Experimental results and associated statistics have indicated that the proposed algorithm provides a significant improvement over many other well-known sharpener-type filters in the aspects of edge and fine detail preservation as well as minimal signal distortion.

REFERENCES

[1] I. Pitas, *Digital Image Processing Algorithms*, Prentice Hall, Upper Saddle River, NJ, USA, 1993.

[2] W. K. Pratt, *Digital Image Processing*, John Wiley & Sons, New York, NY, USA, 1978.

[3] P. Maragos, “Morphological filtering for image enhancement and feature detection,” in *The Image and Video Processing Handbook*, A. C. Bovik, Ed., pp. 135–156, Academic Press, New York, NY, USA, 2005.

[4] T. A. Mahmoud and S. Marshall, “Threshold decomposition driven adaptive morphological filter for image sharpening,” in *Proceedings of the 2nd International Conference on Computer Vision Theory and Applications (VISAPP ’07)*, pp. 40–45, Barcelona, Spain, March 2007.

[5] J. P. Fitch, E. J. Coyle, and N. C. Gallagher Jr., “Median filtering by threshold decomposition,” *IEEE Transactions on Acoustics, Speech, and Signal Processing*, vol. 32, no. 6, pp. 1183–1188, 1984.

[6] G. R. Arce, “A general weighted median filter structure admitting negative weights,” *IEEE Transactions on Signal Processing*, vol. 46, no. 12, pp. 3195–3205, 1998.

[7] J. L. Paredes and G. R. Arce, “Stack filters, stack smoothers, and mirrored threshold decomposition,” *IEEE Transactions on Signal Processing*, vol. 47, no. 10, pp. 2757–2767, 1999.

[8] M. Sharifi, M. Fathy, and M. T. Mahmoudi, “A classified and comparative study of edge detection algorithms,” in *Proceedings of International Conference on Information Technology: Coding and Computing (ITCC ’02)*, pp. 117–120, Las Vegas, Nev, USA, April 2002.

[9] T. Law, H. Itoh, and H. Seki, “Image filtering, edge detection, and edge tracing using fuzzy reasoning,” *IEEE Transactions on Pattern Analysis and Machine Intelligence*, vol. 18, no. 5, pp. 481–491, 1996.

[10] C.-C. Kang and W.-J. Wang, “A novel edge detection method based on the maximizing objective function,” *Pattern Recognition*, vol. 40, no. 2, pp. 609–618, 2007.

[11] S. Mallat and S. Zhong, “Characterization of signals from multiscale edges,” *IEEE Transactions on Pattern Analysis and Machine Intelligence*, vol. 14, no. 7, pp. 710–732, 1992.

[12] D. Heric and D. Zazula, “Combined edge detection using wavelet transform and signal registration,” *Image and Vision Computing*, vol. 25, no. 5, pp. 652–662, 2007.

[13] Y. Zhai and X. Liu, “Adaptive edge detection based on multiscale wavelet features,” in *Proceedings of the 6th World Congress on Intelligent Control and Automation (WCICA ’06)*, vol. 2, pp. 10289–10293, Dalian, China, June 2006.

[14] J. M. Prewitt, “Object enhancement and extraction,” in *Picture Processing and Psychopictorics*, pp. 75–149, Academic Press, New York, NY, USA, 1970.

[15] R. Zhang, G. Zhao, and L. Su, “A new edge detection method in image processing,” in *Proceedings of International Symposium on Communications and Information Technology (ISCIT ’05)*, vol. 2, pp. 430–433, Beijing, China, October 2005.

[16] H. P. Kramer and J. B. Bruckner, "Iterations of a non-linear transformation for enhancement of digital images," *Pattern Recognition*, vol. 7, no. 1-2, pp. 53–58, 1975.

[17] J. M. Lester, J. F. Brenner, and W. D. Selles, "Local transforms for biomedical image analysis," *Computer Graphics and Image Processing*, vol. 13, no. 1, pp. 17–30, 1980.

[18] J. Serra, *Image Analysis and Mathematical Morphology, Vol. I*, Academic Press, London, UK, 1982.

[19] J. G. M. Schavemaker, M. J. T. Reinders, J. J. Gerbrands, and E. Backer, "Image sharpening by morphological filtering," *Pattern Recognition*, vol. 33, no. 6, pp. 997–1012, 2000.

[20] F. Meyer and J. Serra, "Contrasts and activity lattice," *Signal Processing*, vol. 16, no. 4, pp. 303–317, 1989.

[21] F. Y. Shih and O. R. Mitchell, "Threshold decomposition of gray-scale morphology into binary morphology," *IEEE Transactions on Pattern Analysis and Machine Intelligence*, vol. 11, no. 1, pp. 31–42, 1989.

[22] M. Fischer, J. L. Paredes, and G. R. Arce, "Weighted median image sharpeners for the World Wide Web," *IEEE Transactions on Image Processing*, vol. 11, no. 7, pp. 717–727, 2002.

[23] R. C. Hardie and C. G. Boncelet, "LUM filters: a class of rank-order-based filters for smoothing and sharpening," *IEEE Transactions on Signal Processing*, vol. 41, no. 3, pp. 1061–1076, 1993.

[24] T. C. Aysal and K. E. Barner, "Quadratic weighted median filters for edge enhancement of noisy images," *IEEE Transactions on Image Processing*, vol. 15, no. 11, pp. 3294–3310, 2006.

[25] S. Thurnhofer and S. K. Mitra, "A general framework for quadratic Volterra filters for edge enhancement," *IEEE Transactions on Image Processing*, vol. 5, no. 6, pp. 950–963, 1996.

[26] K. Ghosh, S. Sarkar, and K. Bhaumik, "Proposing new methods in low-level vision from the Mach band illusion in retrospect," *Pattern Recognition*, vol. 39, no. 4, pp. 726–730, 2006.

[27] Z. Wang, A. C. Bovik, H. R. Sheikh, and E. P. Simoncelli, "Image quality assessment: from error visibility to structural similarity," *IEEE Transactions on Image Processing*, vol. 13, no. 4, pp. 600–612, 2004.

[28] G.-H. Chen, C.-L. Yang, L.-M. Po, and S.-L. Xie, "Edge-based structural similarity for image quality assessment," in *Proceedings of IEEE International Conference on Acoustics, Speech, and Signal Processing (ICASSP '06)*, vol. 2, pp. 933–936, Toulouse, France, May 2006.